Mechanics Research Communications 103 (2020) 103457

Contents lists available at ScienceDirect

Mechanics Research Communications

journal homepage: www.elsevier.com/locate/mechrescom

Surface growth on a deformable spherical substrate

Rami Abi-Akl[a], Tal Cohen[a,b,*]

[a] Department of Mechanical Engineering, Massachusetts Institute of Technology, Cambridge, MA 02139, United States
[b] Department of Civil and Environmental Engineering, Massachusetts Institute of Technology, Cambridge, MA 02139, United States

ARTICLE INFO

Article history:
Received 24 July 2019
Revised 8 October 2019
Accepted 18 November 2019
Available online 29 November 2019

Keywords:
Universal path
Driving force
Surface growth

ABSTRACT

Kinetics of surface growth with coupled diffusion is studied for the case of growth on a spherical substrate. The considered material system is composed of two species, a solid matrix and a permeating solvent, which can interact by a chemical reaction on the boundaries of the body. It is shown that, for arbitrary substrate curvature, a transient diffusion dominated response is rapidly exhausted before the system arrives at a universal path that is independent of initial conditions. Along this path, the system evolves up to arrival at a steady state, called treadmilling, in which addition and removal of mass are balanced. This result confirms that the universal path, recovered in previous work for growth on a flat rigid substrate, generalizes to additional geometrical settings and also to situations in which the substrate is deformable. The universal path thus facilitates the investigation of the coupling between growth, diffusion and substrate deformation that is induced by buildup of internal stress. This complex coupling is shown to result in a non-monotonic evolution, before arriving at the treadmilling state.

1. Introduction

Surface growth by association or dissociation of material on the boundary of a body is a process that is omnipresent in a variety of natural and engineering contexts. For instance, in nature, surface growth is a key process in growth and remodeling of living tissues [1], development of seashells [2–5], degradation processes [29] and growth of trees [6]. Most available studies of surface growth are based on kinematic assumptions [3,4,7–11]. In that context, Sozio and Yavari [12] have recently presented a geometric theory that captures the nonlinear mechanics and incompatibilities induced by accretion. To couple between the kinematics and the kinetic laws that drive the growth, while requiring conservation of mass, Abi-Akl et al. [13], take advantage of the notion of a reference configuration that can exist in a higher dimensional space, as described for the special case of growth on a spherical substrate in [14], and generalize it to develop a framework for surface growth in a material system composed of two species (i.e. a solid matrix and a solvent) coupled with diffusion. In this framework, the configurational forces that drive association and dissociation are obtained and allow for identification of a thermodynamically consistent kinetic law of growth.

Applying this framework to the case of growth on a flat substrate [13] revealed that before the system arrives at a treadmilling state, in which association and dissociation reactions are balanced, the evolution follows a universal path that is independent of initial conditions. This universal path, which is driven by the harmonious action of surface reaction and diffusion, appears following a rapid transient response that is dominated by diffusion. Being independent of initial conditions, evolution along the universal path was shown to be amenable to analytical investigation. Hence, it was proposed in [13] that taking advantage of this response can simplify the analysis of surface growth in additional, more complex, settings. However, it has not been confirmed that similar evolution would appear in different settings.

In this work, we use the framework developed in [13] to study the evolution of a material grown on a spherical substrate. Beyond the convenience of spherical symmetry to study the effect of substrate curvature, surface growth in spherical settings is also prevalent in nature and thus provides an additional motivation for this study and the specific choice of constitutive relations. For instance, in the context of cell mechanics, polymerization through cross linking of actin filaments to form an elastic gel is a fundamental mechanism that drives cell motility [15–18] which has motivated a number of theoretical studies that focus on this growth pattern [14,19–22]. In this manuscript we first consider a rigid substrate to evaluate the effect of different curvatures on the growth process, then we allow the spherical substrate to deform in response to the buildup of internal stresses and investigate how this coupling between the growth and the substrate curvature influence the response. It will be shown that the universal path appears in both cases, and can be taken advantage of to simplify the solution procedure.

* Corresponding author.
E-mail address: talco@mit.edu (T. Cohen).

https://doi.org/10.1016/j.mechrescom.2019.103457
0093-6413/

2. Problem formulation

The governing equations of surface growth coupled with solvent diffusion, in a general setting, were developed in [13]. Before specializing the formulation to the spherically symmetric problem setting considered in this work, we begin by briefly summarizing that formulation.

In a non-dilute solution, composed of solvent units, we introduce an object of arbitrary shape. On its surface, a chemical reaction promotes association of solvent units to form a solid matrix. That matrix can, in-turn, absorb the solvent and swell to form an aggregate body composed of both a solid matrix and an impregnating solvent. A binding reaction can occur only on the association surface where it is energetically favorable. Consequently, new layers that are formed at the association surface push away the previously formed layers and internal stresses may build up. Dissociation of the material can then occur on the free surface of the grown body. Throughout this process, the surface growth reaction is strongly coupled with solvent diffusion, since conservation of mass requires that the growth reaction is sustained by a continuous supply of solvent units. In this work, we consider each of the species to be separately incompressible, hence conservation of mass translates directly to conservation of volume.

Variables. In the *physical configuration*, the body $\mathcal{R}(t)$ is described by $\mathbf{y}$ and its boundary moves at a velocity $\mathbf{V}$. We denote the solvent volume fraction by $\phi = \phi(\mathbf{y}, t)$, the solvent flux by $\mathbf{j} = \mathbf{j}(\mathbf{y}, t)$, and the Cauchy stress tensor by $\mathbf{T} = \mathbf{T}(\mathbf{y}, t)$. The corresponding variables in the *reference configuration* are described by $\mathbf{x}$ and are denoted by a superimposed $(\,)^{\mathrm{R}}$. The first Piola–Kirchhoff stress tensor is denoted by $\mathbf{S} = \mathbf{S}(\mathbf{x}, t)$.

The correspondence between the physical and the reference configurations relies on the mapping $\mathbf{y} = \hat{\mathbf{y}}(\mathbf{x}, t)$. The deformation gradient is $\mathbf{F}(\mathbf{x}, t) = \partial\hat{\mathbf{y}}(\mathbf{x}, t)/\partial\mathbf{x}$, and the volume ratio is $J(\mathbf{x}, t) = \det(\mathbf{F}(\mathbf{x}, t))$, with the particle velocity given by[1] $\mathbf{v}(\mathbf{x}, t) = \partial\hat{\mathbf{y}}(\mathbf{x}, t)/\partial t$. The boundary velocities in the current and reference configurations are related by

$$\mathbf{V} = \mathbf{F}\mathbf{V}^{\mathrm{R}} + \mathbf{v}, \tag{1}$$

and field variables in the current and reference configurations are related through the following transformations: $\phi^{\mathrm{R}} = J\phi$, $\mathbf{j}^{\mathrm{R}} = J\mathbf{F}^{-1}\mathbf{j}$, and $\mathbf{S} = J\mathbf{T}\mathbf{F}^{-\mathrm{T}}$. The following formulation takes advantage of both configurations as they become useful.

Bulk governing equations. In the physical configuration, species balance and conservation of volume result in the compact set of equations

$$\frac{\partial\phi}{\partial t} + \operatorname{div}(\phi\mathbf{v} + \mathbf{j}) = 0, \quad \operatorname{div}(\mathbf{v} + \mathbf{j}) = 0, \quad J = \frac{1}{1-\phi}, \tag{2}$$

where the latter two field equations assure conservation of each separately incompressible species in any subregion of the body. The former equation relates the volume ratio of the solid matrix and the solvent volume fraction. In absence of body forces, mechanical equilibrium implies $\operatorname{div}\mathbf{T} = \mathbf{0}$, (with $\mathbf{T} = \mathbf{T}^{\mathrm{T}}$). Note that in deriving $(2)_3$ the undeformed configuration of the solid has been chosen as the dry state (for which $\phi = 0$). In the reference configuration, conservation equations simplify to the form

$$\dot{\phi}^{\mathrm{R}} + \operatorname{Div}\left(\mathbf{j}^{\mathrm{R}}\right) = 0, \quad J = 1 + \phi^{\mathrm{R}}, \tag{3}$$

and mechanical equilibrium reads $\operatorname{Div}\mathbf{S} = \mathbf{0}$, (with $\mathbf{S}\mathbf{F}^{\mathrm{T}} = \mathbf{F}\mathbf{S}^{\mathrm{T}}$). We also make use of the relation[2]

$$\frac{1}{J^2}\frac{\partial J}{\partial t} = \operatorname{div}\left(\frac{\mathbf{v}}{J}\right). \tag{4}$$

[1] For simplicity, we will use the same notation, J, and $\mathbf{v}$ for functions expressed in terms of the reference configuration coordinates, $(\mathbf{x}, t)$, and in terms of the physical configuration coordinates, $(\mathbf{y}, t)$.

[2] This relation can be derived from the commonly used identity $\dot{J} = J \operatorname{div}\mathbf{v}$.

Constitutive assumptions. Assuming that the energetic state of a material unit relies on both the elastic deformation of the matrix and the solvent concentration, we take the free energy per unit referential volume to have the form $\psi = \psi(\mathbf{F}, \phi^{\mathrm{R}})$. Using the Coleman–Noll methodology on the dissipation rate, constitutive relations for the stresses and for the chemical potential μ can be obtained and a thermodynamically consistent kinetic law for diffusion of solvent can be chosen to satisfy the non-negativity of the dissipation rate, i.e. $\mathbf{j}^{\mathrm{R}} \cdot \operatorname{Grad}\mu \leq 0$. Through this procedure, the hydrostatic pressure p arises as a reaction to the volume conservation constraint and is constitutively indeterminate.

Interface equations and growth kinetics. In writing the conditions for conservation of volume across the boundary of the growing body, the motion of the boundary ($\mathbf{V}$) and the flux should be considered to write[3]

$$-\mathbf{j}^{+} \cdot \mathbf{n} + \mathbf{V} \cdot \mathbf{n} = -\mathbf{j}^{-} \cdot \mathbf{n} + (\mathbf{V} - \mathbf{v}) \cdot \mathbf{n}. \tag{5}$$

Additionally, we require continuity of chemical potential across the boundary, i.e. $\mu^{+} = \mu^{-}$, which is consistent with a Fick's type diffusion law. Displacement and stress boundary conditions are also applied on the growing body.

Finally, it was shown in [13] that the driving force of growth acting on the boundary can be written as

$$f = \mathbf{S}\mathbf{n}^{\mathrm{R}} \cdot \mathbf{F}\mathbf{n}^{\mathrm{R}} + \Delta\psi + \mu J, \tag{6}$$

where $\Delta\psi = \psi^{+} - \psi^{-}$ is the latent energy of the growth reaction. The growth rate is the thermodynamic conjugate to the driving force. The two can be related through a kinetic law of the form $\mathrm{V}^{\mathrm{R}} = \mathcal{G}(f)$, which obeys the dissipation inequality if $f\mathcal{G}(f) \geq 0$.

3. Growth on a spherical surface

We now apply the theory to the specific problem of growth on a rigid, impermeable and spherical surface of radius r_a. We will first write the formulation considering a rigid growth surface of constant curvature. It will be shown that in absence of inertial effects the formulation can be directly applied to consider situations in which the growth surface can deform in response to the growth process that leads to accumulation of residual stresses. Ultimately, the goal is to describe the time evolution of the growing body and to identify a treadmilling response, shall it exist.

3.1. Sperical problem setting

The physical configuration is described by spherical system of coordinates (r, θ, φ), where the association surface is at the constant location $r = r_a$ and the dissociation surface is at $r = r_d(t)$, as shown in Fig. 1. Growth is initiated at time $t = 0$. For any $t > 0$, the growing body manifold occupies the region $r \in [r_a, r_d(t)]$, $\theta \in [0, \pi]$, and $\varphi \in [0, 2\pi]$.

As shown in [14] and further discussed in [13], within a four-dimensional space, the material manifold occupies the surface of a hyper-cylinder whose base is a spherical surface of undeformed radius R (note the difference in notation $\mathcal{R}$ which denotes the body), described by the coordinates $\Theta \in [0, \pi]$, and $\Phi \in [0, 2\pi]$. The axis of the hyper-cylinder spans along the Z coordinate, and its caps move to accommodate association or dissociation, such that the association surface is given by $Z = Z_a(t)$, and the dissociation surface is given by $Z = Z_d(t)$. Thus, the reference configuration can be described by the set of coordinates (Z, Θ, Φ). The radius of the base can be obtained by considering the tangential

[3] The superscripts '+' and '−' on a quantity denote its limiting values on the outer and inner side of the, respectively.

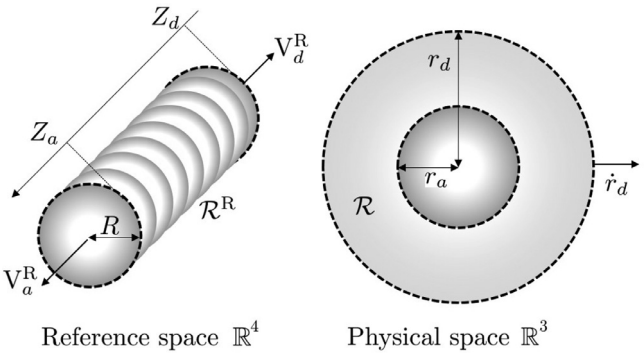

Fig. 1. Continuum representation of a body growing on a spherical substrate and corresponding boundary velocities in both the reference and the physical spaces.

stretch imposed on the layer as it grows on association surface[4] $-\lambda_0$ to write $R = r_a/\lambda_0$. Due to spherical symmetry, the mapping between the reference and current configurations can be written as $(r, \theta, \varphi) = (\hat{r}(Z, t), \Theta, \Phi)$. The principal stretches in the radial and circumferential directions and the swelling ratio are thus

$$\lambda_r = \frac{\partial r}{\partial Z}, \quad \lambda_\theta = \lambda_\varphi = \frac{r}{R}, \quad J = \lambda_r \lambda_\theta^2 = \frac{\partial r}{\partial Z}\left(\frac{r}{R}\right)^2, \tag{7}$$

respectively.

Motion occurs only in the radial direction in the physical configuration, hence the material velocity and flux can be written as $\mathbf{v} = \mathrm{v}(r)\mathbf{e}_r$ and $\mathbf{j} = \mathrm{j}(r)\mathbf{e}_r$, where $\mathrm{v}(r) = \partial \hat{r}/\partial t$. In this setting, the velocity of the association and dissociation boundaries in the physical configuration are $\mathbf{V}_a = \mathbf{0}$ and $\mathbf{V}_d = \dot{r}_d(t)\mathbf{e}_r$, respectively, and in the reference configuration

$$\mathbf{V}_a^R = -\mathrm{V}_a^R \mathbf{e}_Z \quad \text{and} \quad \mathbf{V}_d^R = \mathrm{V}_d^R \mathbf{e}_Z, \tag{8}$$

where $\mathrm{V}_a^R = -\dot{Z}_a$ and $\mathrm{V}_d^R = \dot{Z}_d$ are the association and dissociation rates, respectively. From here on the subscripts $(\,)_a$ and $(\,)_d$ denote values at the association and dissociation boundaries (i.e. r_a and r_d), respectively.

Let $\ell(t)$ denote the thickness of the body in the physical configuration, it can be expressed as

$$\ell(t) = r_d(t) - r_a. \tag{9}$$

Similarly, let $\ell^R(t)$ denote the thickness of the growing layer in the reference configuration, that we shall refer to as the *dry thickness*, it can be written as

$$\ell^R(t) = Z_d(t) - Z_a(t). \tag{10}$$

By combination of (8) and (10), the dry thickness evolves at the rate

$$\dot{\ell}^R = \mathrm{V}_a^R + \mathrm{V}_d^R. \tag{11}$$

Now, specializing the conservation equation $(2)_2$, and integrating it, while employing the condition that association surface is impermeable, we obtain the simplified form

$$\mathrm{v} + \mathrm{j} = 0, \quad r_a < r < r_d(t). \tag{12}$$

We also specialize Eq. (4) to the present spherically symmetric setting to write

$$\frac{\partial J}{\partial t} = \frac{J^2}{r^2}\frac{\partial}{\partial r}\left(\frac{r^2}{J}\mathrm{v}\right). \tag{13}$$

[4] This is a property of the growth surface that can be determined for example by the distribution of binding sites; it represent the in-plane predeformation of the newly associated material.

Using a diffusion law of the general form $\mathbf{j}^R = -\mathbf{M}(\mathbf{F}, \phi^R)\,\mathrm{Grad}\,\mu$ with Eq. (12) and, specializing to the present setting, we can express the velocity v as

$$\mathrm{v} = \frac{\lambda_r^2}{J} M_{11} \frac{\partial \mu}{\partial r}, \tag{14}$$

where $M_{11} > 0$ is the (1,1)-component of the positive semi-definite mobility tensor $\mathbf{M}$.

Mechanical equilibrium implies

$$\frac{\partial \mathrm{T}_r}{\partial r} + \frac{2}{r}(\mathrm{T}_r - \mathrm{T}_\theta) = 0, \tag{15}$$

where T_r and T_θ are the radial and tangential components of the Cauchy stress tenor. Considering situations in which the dissociation surface is stress free, we can write the boundary condition $\mathrm{T}_r(r_d) = 0$.

In this specific spherical setting, assuming isotropy, we can write the Helmholtz free energy as a function of the principal stretches and the solvent volume fraction in the form $\psi = \psi(\lambda_r, \lambda_\theta, \lambda_\varphi, \phi^R)$. The principal components of the Cauchy stress tensor, and the chemical potential thus read

$$\mathrm{T}_r = \frac{1}{J}\frac{\partial \psi}{\partial \lambda_r}\lambda_r - p, \quad \mathrm{T}_\theta = \frac{1}{J}\frac{\partial \psi}{\partial \lambda_\theta}\lambda_\theta - p, \quad \mu = \frac{\partial \psi}{\partial \phi^R} + p, \tag{16}$$

respectively. Substituting (16) in (15), we can write

$$\frac{\partial p}{\partial r} = \frac{\partial}{\partial r}\left(\frac{1}{J}\frac{\partial \psi}{\partial \lambda_r}\lambda_r\right) + \frac{2}{rJ}\left(\frac{1}{J}\frac{\partial \psi}{\partial \lambda_r}\lambda_r - \frac{1}{J}\frac{\partial \psi}{\partial \lambda_\theta}\lambda_\theta\right). \tag{17}$$

Recall that p, the hydrostatic pressure, arises as a response to the incompressibility constraint.

Using relations $(3)_2$ and (7), all the relevant physical quantities, that depend on ϕ^R, λ_r and λ_θ, can be rewritten in terms of r and J only: $\psi(r, J)$, $\mathbf{T}(r, J)$, $p(r, J)$ and $\mu(r, J)$. Additionally, substituting the derivative of $(16)_3$ in Eqs. (12) and (14) we can write

$$\frac{r^2}{J}\mathrm{v} = \mathcal{L}\left(r, J, \frac{\partial J}{\partial r}\right), \tag{18}$$

where for brevity, we specify the function $\mathcal{L}$ in the next section for a specific constitutive response.

Now, returning to the relation for the driving force (6), we find that in contrast to the case of growth on a flat surface (considered in [13]), the term $\mathbf{S}\mathbf{n}^R$ does not vanish on the association boundary. Hence, stresses play a role in determining the driving force of growth, which in spherical symmetry reads

$$f = J\mathrm{T}_r + \Delta\psi + J\mu. \tag{19}$$

On the association surface the latent energy of growth has the form $\Delta\psi = \psi_a - \psi^-$, with ψ_a denoting the chemical binding potential [13]. Consequently, since $\mathrm{V}_a^R = \mathcal{G}(f_a)$ and $\mathrm{V}_d^R = \mathcal{G}(f_d)$, the association and dissociation rates can be expressed in terms of r_a, J_a, r_d and J_d. Thus the coupling between surface growth and swelling is generated by the dependence of the association and dissociation rates on the local values of the swelling ratio J.

For a complete formulation of the initial-boundary value problem, there remains the definition of additional boundary conditions. On the dissociation boundary $(r = r_d(t))$, the continuity of chemical potential implies

$$\mu(r_d, J_d) = \mu_0, \tag{20}$$

thus resulting in an implicit equation relating J_d and r_d. By the kinematic relation (1), the particle velocity at association and dissociation boundaries are

$$\mathrm{v}_a = \frac{R^2}{r_a^2} J_a \mathrm{V}_a^R \quad \text{and} \quad \mathrm{v}_d = \dot{r}_d - \frac{R^2}{r_d^2} J_d \mathrm{V}_d^R, \tag{21}$$

respectively. The boundary condition on the association surface is thus obtained by combination of (18) and $(21)_1$.

In summary, the initial-boundary value problem can be written in terms of the swelling field $J(r, t)$ in the physical configuration as

$$\begin{cases} \dfrac{\partial J}{\partial t} = \dfrac{J^2}{r^2}\dfrac{\partial}{\partial r}\left(\mathcal{L}\left(r, J, \dfrac{\partial J}{\partial r}\right)\right), & r_a \le r \le r_d(t), \\ \mu(r_d, J_d) = \mu_0, & r = r_d(t), \\ \mathcal{L}\left(r, J, \dfrac{\partial J}{\partial r}\right) = R^2 \mathrm{V}_a^{\mathrm{R}}(r_a, J_a), & r = r_a, \\ J(r, 0) = J_0(r), & t = 0, \end{cases} \tag{22}$$

where the moving boundary obeys

$$\begin{cases} \dot{r}_d = \dfrac{J_d}{r_d^2}\left[\mathcal{L}\left(r_d, J_d, \dfrac{\partial J}{\partial r}|_{r=r_d}\right) + R^2 \mathrm{V}_d(r_d, J_d)\right] \\ r_d(0) = r_0 \end{cases} \tag{23}$$

It is important to note that the system is fully described at a given time by the thickness and swelling ratio, $(\ell(t), J(r, t))$ in the physical configuration, which can be directly translated to determine $(\ell^{\mathrm{R}}(t), J(Z, t))$ in the reference configuration. This initial-boundary value problem is written here for a general material system composed of two species (a solid matrix and a solvent). Next, to evaluate solutions we will consider a specific constitutive model.

3.2. Specific constitutive model

Considering a growth reaction of polymerization to form a polymer network permeated by a solvent, we employ a Helmholtz free energy following the Flory and Rehner [23] approach as in [13,24–26], we write

$$\begin{aligned} \psi(\mathbf{F}, J) = {} & (J-1)\psi_0 + \frac{kT}{\nu}(J-1)\left[\ln\left(1-\frac{1}{J}\right) + \frac{\chi}{J}\right] \\ & + \frac{NkT}{2}\left(|\mathbf{F}|^2 - 3 - 2\ln(\det \mathbf{F})\right). \end{aligned} \tag{24}$$

Here we have readily substituted $\phi^{\mathrm{R}} = J - 1$. Next, using (16), the principal stress components thus read

$$\mathrm{T}_r = \frac{NkT}{J}\left(\frac{R^4}{r^4}J^2 - 1\right) - p, \quad \mathrm{T}_\theta = \mathrm{T}_\phi = \frac{NkT}{J}\left(\frac{r^2}{R^2} - 1\right) - p, \tag{25}$$

and the chemical potential is

$$\mu = \mu_0 + \frac{kT}{\nu}\left[\ln\left(1-\frac{1}{J}\right) + \frac{1}{J} + \frac{\chi}{J^2}\right] + p. \tag{26}$$

The solvent diffusion within the solid matrix is assumed to follow the classical model [27], hence (14) translates to

$$\mathrm{v} = \frac{D\nu}{kT}\phi\ \frac{\partial \mu}{\partial r}, \tag{27}$$

where D is the diffusion coefficient.

As in [13], the growth function is taken of the Arrhenius form

$$\mathcal{G}(f) = \frac{b}{2}\left(e^{\frac{\nu f}{kT}} - e^{-\frac{\nu f}{kT}}\right) = b\sinh\left(\frac{\nu f}{kT}\right). \tag{28}$$

Now, replacing (25) in the equilibrium equation (15), the pressure gradient is simplified to the form

$$\frac{\partial p}{\partial r} = NkT\left[-2\left(\frac{R^4}{r^5}J + \frac{r}{R^2 J}\right) + \left(\frac{R^4}{r^4} + \frac{1}{J^2}\right)\frac{\partial J}{\partial r}\right]. \tag{29}$$

From (25), the traction free condition at r_d implies

$$p(r_d) = \frac{NkT}{J_d}\left(\frac{R^4}{r^4}J_d^2 - 1\right). \tag{30}$$

Combining the kinetic law (27) with (18) we can write

$$\begin{aligned} \mathcal{L}\left(r, J, \frac{\partial J}{\partial r}\right) = {} & \frac{r^2}{J}D\left(1-\frac{1}{J}\right)\left[\left(N\nu\frac{R^4}{r^4} + \frac{1}{J-1} - \frac{1}{J}\right.\right. \\ & \left.\left. - \frac{1-N\nu}{J^2} - 2\chi\frac{1}{J^3}\right)\frac{\partial J}{\partial r} - 2N\nu\left(\frac{R^4}{r^5}J + \frac{r}{R^2 J}\right)\right]. \end{aligned} \tag{31}$$

Finally, from (26), the continuity of chemical potential at the dissociation boundary is

$$\ln\left(1-\frac{1}{J_d}\right) + \frac{1}{J_d} + \frac{\chi}{J_d^2} + \frac{N\nu}{J_d}\left(\frac{R^4}{r_d^4}J_d^2 - 1\right) = 0. \tag{32}$$

Notice that in contrast to the case of growth on a flat surface, J_d is not constant in time as it depends on r_d that varies with time.

A full description of the material response is thus defined by a set of material parameters (ν, N, χ, ψ_0, D, b). In solving for treadmilling in the next section we will use values of the model parameters within common ranges found in the literature [13,24,26,28]: $\nu = 10^{-28}\,\mathrm{m}^3$, $N = 10^{24}\,\mathrm{m}^{-3}$, $\chi = 0.2$ and $\psi_0 = -4\times10^5\,\mathrm{J m}^{-3}$, and assuming room temperature we have $kT = 4\times10^{-21}\,\mathrm{J}$, $D\nu = 10^{-8}\,\mathrm{m}^2\mathrm{s}^{-1}$ and $b = 10^{-7}\,\mathrm{m s}^{-1}$. While holding these values constant, investigation of the sensitivity of our results will center on the curvature of the growth surface.

4. Results for growth on a rigid substrate

Treadmilling. When addition and removal of mass are balanced, all time derivatives in the current configuration vanish and the system arrives at a treadmilling state. In this steady state, the layer thickness, ℓ (or equivalently ℓ^R), remains constant, although association and dissociation persist. If a treadmilling state exists, the boundary value problem (22) and the associated boundary motion (23) can be solved to determine these thicknesses and the corresponding steady field $\tilde{J}(r)$. The superior $\tilde{(\,)}$ will be used henceforth to denote quantities associated with the treadmilling state, e.g. $\tilde{\ell}$ is the value of ℓ at treadmilling.

According to (11), when addition of solid mass at $r = r_a$ is balanced by the removal of solid mass at $r = r_d$, we can write

$$\mathrm{V}_a^{\mathrm{R}}(r_a, \tilde{J}_a) = -\mathrm{V}_d^{\mathrm{R}}(\tilde{r}_d, \tilde{J}_d), \tag{33}$$

where $\tilde{J}_a = \tilde{J}(r = r_a)$ denotes the steady swelling ratio at the association boundary. Since the association surface is rigid, r_a is constant. Eqs. (20) and (33) are independent, and relate the three unknowns $\tilde{J}_a$, $\tilde{r}_d$ and $\tilde{J}_d$. We thus need to identify a third independent equation to determine all three unknowns. When the time derivatives in the current configuration vanish, it follows from $(22)_1$ and $(22)_3$ that the steady field $\tilde{J}$ obeys the differential equation

$$\mathcal{L}\left(r, \tilde{J}, \frac{\partial \tilde{J}}{\partial r}\right) = R^2 \mathrm{V}_a^{\mathrm{R}}(r_a, \tilde{J}_a), \qquad r_a < r < \tilde{r}_d. \tag{34}$$

Integrating the above relation between r_a and $\tilde{r}_d$, and enforcing $\tilde{J}(r = r_a) = \tilde{J}_a$ and $\tilde{J}(r = r_d) = \tilde{J}_d$ yields an implicit relation between $\tilde{J}_a$, $\tilde{r}_d$ and $\tilde{J}_d$, which, combined with (20) and (33), provides a solution for these three variables. Then, integrating this same relation (34) between r_a and $r \in [r_a, \tilde{r}_d]$, we obtain an implicit relation between the swelling ratio $\tilde{J}$ and the spatial coordinate r.

The pressure throughout the thickness is obtained by integration of Eq. (29) with boundary condition (30) and the stress state can be determined using (25).

To understand the sensitivity of the treadmilling response to the problem geometry, we introduce the curvature $\gamma = 1/r_a$. Let $\tilde{\ell}_0$ denote the treadmilling thickness in the flat surface limit examined in [13], corresponding to $\gamma = 0$. The thickness $\tilde{\ell}_0$ will be used to normalize lengths. We thus define the normalized radius $r_a^* = r_a/\tilde{\ell}_0$, the normalized curvature $\gamma^* = 1/r_a^*$, and the normalized treadmilling thickness for a given curvature $\tilde{\ell}^* = \tilde{\ell}/\tilde{\ell}_0$. We will

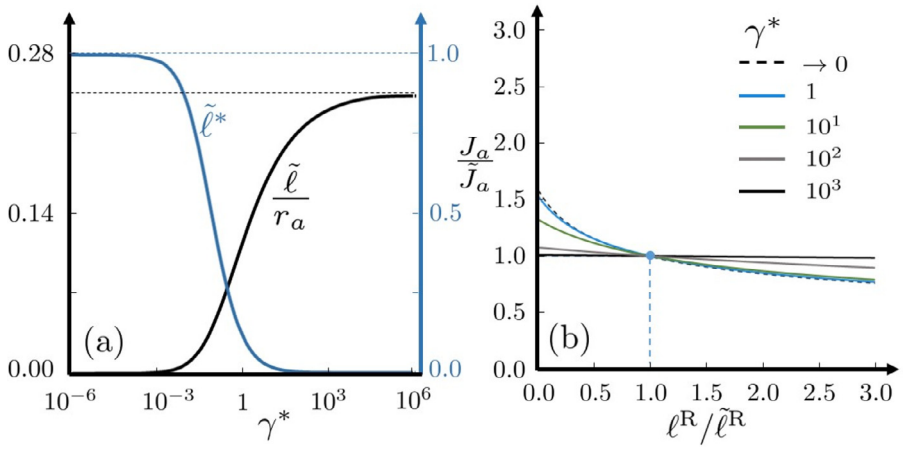

Fig. 2. (a) Dependence of the treadmilling thickness on the normalized curvature of the growth surface represented on a logarithmic scale shown using two different normalizations. (b) Effect of γ^* on the universal path. The universal paths determined by numerical simulations are indistinguishable from the analytical relation obtained by integration of (35) in the reference frame.

focus our discussion in this section to the sensitivity of the growth process to the substrate curvature. It has been confirmed that the sensitivity to model parameters λ_0 and ψ_a is comparable to those observed for growth on a flat surface [13]. In all of the results presented in this manuscript we will use representative values from [13], (i.e. $\lambda_0 = 4.96$ and $\psi_a/(kT/\nu) = -0.325$).

Fig. 2 (a) shows the sensitivity of the normalized treamilling thickness to the curvature of the growth surface (shown in a logarithmic scale). Focusing on the blue curve, it is observed that for $\gamma^* \to 0$, the solution converges towards the flat surface limit $\tilde{\ell}^* \to 1$. As γ^* increases, $\tilde{\ell}^*$ vanishes. This behavior is due to transition from a diffusion-limited to a stress-limited response for higher curvatures.

To better characterize the treadmilling response for growth surfaces with $\gamma^* \gg 1$, we examine the product $\gamma\tilde{\ell} = \tilde{\ell}/r_a$ that is represented by the black curve in Fig. 2(a). It is shown that for increasing curvatures the ratio between the grown thickness and the substrate radius arrives at an asymptotic maximum. Essentially, even though the treamilling thickness vanishes as the radius of the growth surface vanishes, the geometric ratio becomes more significant for smaller growth surfaces.

Evolution towards treadmilling. Although the analysis of the treadmilling response provides us a means for analytical investigation of the sensitivities of the growth process, it is also insightful to examine the evolution of growth prior to its arrival at a treadmilling state. Hence, the initial boundary value problem (22) is solved for various initial conditions, employing a specialized finite difference method that employs two integration time scales, to track both the moving boundaries and the diffusion mechanism [13].

By examining numerical solutions for growth starting from different initial conditions (conducted using a finite difference scheme that employs two integration timescales) we find that the system undergoes a two stage evolution: first, a rapid diffusion-dominated regime in which changes in dry thickness are negligible, then a sharp change in the evolution trend towards a universal path, which is independent of initial conditions. Along this path surface growth and solvent diffusion are fully coupled and act harmoniously to determine the evolution. Universal paths for layers grown on substrates with different curvatures are shown in Fig. 2(b) in the form of phase maps exhibiting the swelling ratio at the association surface as a function of the dry length of the layer. Both variables are normalized by their treadmilling value, so that for all curves treadmilling appears at the point (1,1). If shown, the diffusion dominated response would appear in this map as a straight vertical line connecting some initial state, to the universal path. This response is identical to what has been observed for the limiting case of growth on a flat surface [13]. Here we confirm that the existence of a universal path generalizes to more complex growth geometries, which involve buildup of residual stresses.

While evolving along the universal path, the body is at a quasi-equilibrated state in which the time derivative on the left hand side of $(22)_1$ becomes negligible, although the thickness continues to evolve. Dropping this time derivative and using the boundary condition $(22)_3$ leads to

$$\mathcal{L}\left(r, J, \frac{\partial J}{\partial r}\right) = R^2 \mathrm{V}_a^{\mathrm{R}}(r_a, J_a), \qquad r_a \le r \le r_d(t), \tag{35}$$

which is different from (34), in allowing for time dependent r_d and J_a which have not yet arrived at their treadmilling value. By integration of the above relation between Z_a and Z_d, using the relation in $(7)_3$ for the swelling ratio, provides an implicit relation between ℓ^{R} and J_a which describes the of the universal path in the (ℓ^{R}, J_a)-plane. Universal curves obtained directly using this approach, are identical to the ones obtained numerically (Fig. 2). Note that at the limit $\gamma^* \to 0$, the present analysis retrieves the curve obtained in [13] for growth on a flat surface.

5. Growth on a deformable substrate

We now show that the previous analysis of growth on a rigid sphere can be extended to account for deformability of the growth surface. We thus consider situations in which the substrate radius, $r_a(t)$, can change throughout the growth process, as a response to the buildup of internal stresses in the growing body. For simplicity, we restrict our attention to situations in which the dry, stress free, configuration of a spherical layer has the same radius R as the unloaded substrate. Hence, the circumferential stretch of the layer formed at the association surface can vary, as is given by $\lambda_0(t) = r_a(t)/R$. Essentially, this assumption implies that the number of binding sites on the substrate remains constant as it deforms. For the analysis we choose $R = DN\nu/b$, which as shown in [13], is a characteristic length scale, and will allow us to remain in the stress-limited regime in this analysis.

When on the universal path, for a given r_a, the system is fully characterized by ℓ^{R}, through the bijection that exists between ℓ^{R} and J_a that is the universal path described in the previous section. Thus, when we consider a deformable sphere, we will take advantage of the universal paths associated with different values of r_a (or equivalently γ^*), and will complement them by tracking the

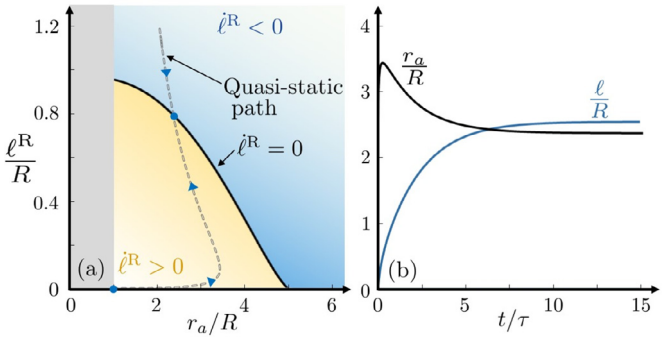

Fig. 3. (a) Quasi-static evolution path shown by the dashed–dotted line in the $(r_a, \ell^R)/R$. Black line distinguishes between regions of positive and negative values of the macroscopic growth rate $\dot{\ell}^R$. (b) Time evolution of ℓ and r_a starting from inception. The time has been normalized by the characteristic time-scale $\tau = R/b = DN\nu/b^2$.

evolution in the (r_a, ℓ^{R})-plane to describe the variety of problem configurations. The problem can be fully described by determining the four variables: $r_a(t)$, $r_d(t)$, $J_a(t)$ and $J_d(t)$.

The procedure is as follows: for a given point (r_a, ℓ^{R}) there exists a unique J_a, as determined from the universal path (35). There remains r_d and J_d, that can be determined by requiring continuity of chemical potential (20). Then the remaining unknown is identified by imposing the continuity of radial stresses at the association boundary, which is a result of the mechanical response of the substrate relating its deformation to the radial traction (which will be elaborated in the next section). Ultimately, the system evolution will be along the quasi-static path, in the direction that is coherent with the sign of $\dot{\ell}^R$.

Mechanical boundary condition. The radial stress applied to the growing body at $r = r_a(t)$ equals the radial stress applied on the substrate to achieve mechanical equilibrium. Namely, we have the boundary condition $T_r(r_a) = \sigma_r(r_a)$, where the function $\sigma_r(r_a)$ is a property of the substrate, which can be thought of as a deformable shell. For a given ℓ^{R}, this boundary condition leads to a unique r_a. Thus, $r_a(\ell^{\mathrm{R}})$ defines a *quasi-static* path that the system has to be on to achieve both swelling and mechanical equilibrium. In Fig. 3, we represent this quasi-static path in the (r_a, ℓ^{R})-plane, using a dashed line. On this path, the association and dissociation rates are not necessarily balanced, hence treadmilling is not ensured. To obtain the results of Fig. 3 we have used a simple linear law of the form $\sigma_r(r_a) = A(r_a - R)$, with $A = 2 \cdot 10^4 \mathrm{Pa.m}^{-1}$. The results hold qualitatively for higher order laws.

Treadmilling. When the substrate is deformable, the treadmilling response is characterized by (i) balance between association and dissociation, and (ii) vanishing time derivatives in the current configuration. Thus at treadmilling, both radii $\tilde{r}_a$ and $\tilde{r}_d$ are constant, as well as dry thickness $\tilde{\ell}^{\mathrm{R}}$ and swelling throughout the thickness $\tilde{J}(r)$. For each bead radius r_a (or equivalently γ^*), there exists a unique treadmilling dry thickness ℓ^{R} defined from the universal paths in the previous section. In Fig. 3(a), we represent in the (r_a, ℓ^{R})-plane two different domains, characterized by $\mathrm{V}_a^{\mathrm{R}} < -\mathrm{V}_d^{\mathrm{R}}$ and $\mathrm{V}_a^{\mathrm{R}} > -\mathrm{V}_d^{\mathrm{R}}$, separated by a line where $\mathrm{V}_a^{\mathrm{R}} = -\mathrm{V}_d^{\mathrm{R}}$. In this plane, a treadmilling state must fall on this specific curve. Therefore treadmilling must occur at the intersection between the two curves in Fig. 3(a).

Evolution from inception to treadmilling. Employing the quasi-static path and extending it to capture the formation of the very first layer, at the limit where $r_a/R \to 1$ and $\ell^{\mathrm{R}}/\tilde{\ell}^{\mathrm{R}} \to 0$. Using time integration of the quasi-static solution (using (33) and (35) while allowing for time variation of r_a), we show in Fig. 3(b) the evolution of substrate radius and the grown thickness over time. The thickness increases monotonically, whereas the substrate radius undergoes an initial overshoot before converging towards its treadmilling value. This is due to competition between build-up of stresses and diffusion, which act at different characteristic times. At onset, rapid diffusion leads to a fast increase in radius, which is later countered by stresses that build-up due to the thickening of the layer.

The initial layers formed at the association surface of radius r_a close to R are dense ($\lambda_0 = 1$) and thus have a propensity to swell and increase the tangential stretch (thus increasing r_a). This first phase of the evolution is limited by diffusion. Then, as the growing body thickens, stresses start building up and the grown layer pushes against the substrate thus reducing its radius. Ultimately, the final treadmilling reached is a balance between swelling effects, growth reactions and residual stresses.

Concluding statement. We have shown, in the spherical setting, how the harmonious interplay between surface growth, diffusion effects and mechanical constraints governs the growth of a body and the deformation of the substrate on which it grows. This study can be adapted to different scenarios by tuning the constitutive and kinetic parameters, and varying the substrate properties. Further computational models will allow to extend it to arbitrary geometries.

Declaration of Competing Interest

There are no conflicts of interest to declare.

References

[1] G.A. Ateshian, On the theory of reactive mixtures for modeling biological growth, Biomech. Model. Mechanobiol. 6 (2007) 423–445.
[2] D.W. Thompson, On Growth and Form, 1917, 1970.
[3] R. Skalak, D. Farrow, A. Hoger, Kinematics of surface growth, J. Math. Biol. 35 (1997) 869–907.
[4] D.E. Moulton, A. Goriely, R. Chirat, Mechanical growth and morphogenesis of seashells, J. Theor. Biol. 311 (2012) 69–79.
[5] A. Goriely, The Mathematics and Mechanics of Biological Growth, Springer, 2017.
[6] R.R. Archer, Growth Stresses and Strains in Trees, 3, Springer Science & Business Media, 2013.
[7] R. Skalak, G. Dasgupta, M. Moss, E. Otten, P. Dullemeijer, H. Vilmann, Analytical description of growth, J. Theor. Biol. 94 (1982) 555–577.
[8] A. Menzel, E. Kuhl, Frontiers in growth and remodeling, Mech. Res. Commun. 42 (2012) 1–14.
[9] G. Zurlo, L. Truskinovsky, Printing non-Euclidean solids, Phys. Rev. Lett. 119 (2017) 048001.
[10] G. Zurlo, L. Truskinovsky, Inelastic surface growth, Mech. Res. Commun. 93 (2018) 174–179.
[11] F. Sozio, A. Yavari, Nonlinear mechanics of surface growth for cylindrical and spherical elastic bodies, J. Mech. Phys. Solids 98 (2017) 12–48.
[12] F. Sozio, A. Yavari, Nonlinear mechanics of accretion, J. Nonlinear Sci. 29 (4) (2019) 1813–1863.
[13] R. Abi-Akl, R. Abeyaratne, T. Cohen, Kinetics of surface growth with coupled diffusion and the emergence of a universal growth path, Proc. R. Soc. A 475 (2019) 20180465.
[14] G. Tomassetti, T. Cohen, R. Abeyaratne, Steady accretion of an elastic body on a hard spherical surface and the notion of a four-dimensional reference space, J. Mech. Phys. Solids 96 (2016) 333–352.
[15] R. Boujemaa-Paterski, E. Gouin, G. Hansen, S. Samarin, C.L. Clainche, D. Didry, P. Dehoux, P. Cossart, C. Kocks, M.F. Carlier, et al., Listeria protein acta mimics wasp family proteins: it activates filament barbed end branching by ARP2/3 complex, Biochemistry 40 (2001) 11390–11404.
[16] J. Prost, J.-F. Joanny, P. Lenz, C. Sykes, The physics of listeria propulsion, in: Cell Motility, Springer, 2008, pp. 1–30.
[17] K. John, D. Caillerie, P. Peyla, M. Ismail, A. Raoult, J. Prost, C. Misbah, Act-in-based propulsion: Intriguing interplay between material properties and growth processes, in: Cell Mechanics, Chapman and Hall/CRC, 2010, pp. 47–84.
[18] V. Noireaux, R. Golsteyn, E. Friederich, J. Prost, C. Antony, D. Louvard, C. Sykes, Growing an actin gel on spherical surfaces, Biophys. J. 78 (2000) 1643–1654.
[19] T. Cohen, D. Durban, Y.F. Dafalias, Dampening effects on the polymerization rate of actin gel surface growth, Extreme Mech. Lett. 1 (2014) 114–119.
[20] D. Durban, T. Cohen, Y. Dafalias, Solid flow fields and growth of soft solid mass, Proc. IUTAM 12 (2015) 31–41.
[21] Y.F. Dafalias, D.E. Panayotounakos, Z. Pitouras, Stress field due to elastic mass growth on spherical and cylindrical substrates, Int. J. Solids Struct. 45 (2008) 4629–4647.
[22] Y.F. Dafalias, Z. Pitouras, Stress field in actin gel growing on spherical substrate, Biomech. Model. Mechanobiol. 8 (2009) 9–24.

[23] P.J. Flory, J.J. Rehner, Statistical mechanics of cross-linked polymer networks ii. swelling, J. Chem. Phys. 11 (1943) 521–526.
[24] W. Hong, X. Zhao, J. Zhou, Z. Suo, A theory of coupled diffusion and large deformation in polymeric gels, J. Mech. Phys. Solids 56 (2008) 1779–1793.
[25] F.P. Duda, A.C. Souza, E. Fried, A theory for species migration in a finitely strained solid with application to polymer network swelling, J. Mech. Phys. Solids 58 (2010) 515–529.
[26] S.A. Chester, L. Anand, A coupled theory of fluid permeation and large deformations for elastomeric materials, J. Mech. Phys. Solids 58 (2010) 1879–1906.
[27] R.P. Feynman, R.B. Leighton, M. Sands, The Feynman Lectures on Physics, 1, Elsevier, 1963.
[28] Y. Lai, Y. Hu, Probing the swelling-dependent mechanical and transport properties of polyacrylamide hydrogels through AFM-based dynamic nanoindentation, Soft Matter 14 (2018) 2619–2627.
[29] R. Abi-Akl, E. Ledieu, T.N. Enke, O.X. Cordero, T. Cohen, Physics-based prediction of biopolymer degradation, Soft Matter 15 (20) (2019) 4098–4108, doi:10.1039/C9SM00262F.